Supplementary Information

Macroporous Perovskite Nanocrystal Composites for Ultrasensitive Copper Ion Detection

Hanchen Li,[‡a,b] Wenping Yin,[*‡ a,b] Chun Kiu Ng,[a,b] Ruoxi Huang,[a,b] Shengrong Du,[b] Manoj Sharma,[a,b] Bin Li,[a,b] Gangcheng Yuan,[a,c] Monika Michalska,[a,b] Sri Kasi Matta,[a,e] Yu Chen,[d] Naresh Chandrasekaran,[a,b] Salvy Russo,[a,e] Neil R. Cameron,[b,f] Alison M. Funston[a,c] and Jacek J. Jasieniak[*,a,b]

[a] *Australian Research Council Centre of Excellence in Exciton Science, Australia*

[b] *Department of Materials Science and Engineering, Monash University, Clayton, Victoria, 3800, Australia*

[c] *School of Chemistry, Monash University, Clayton, Victoria, 3800, Australia*

[d] *Monash Centre for Electron Microscopy (MCEM), Monash University, Clayton, Victoria, 3800, Australia*

[e] *School of Science, RMIT University, Melbourne, 3000, Australia*

[f] *School of Engineering, University of Warwick, Coventry CV4 7AL, U.K.*

‡*Both authors contributed equally to this work.*

Table of Contents

1. Supplementary Figures

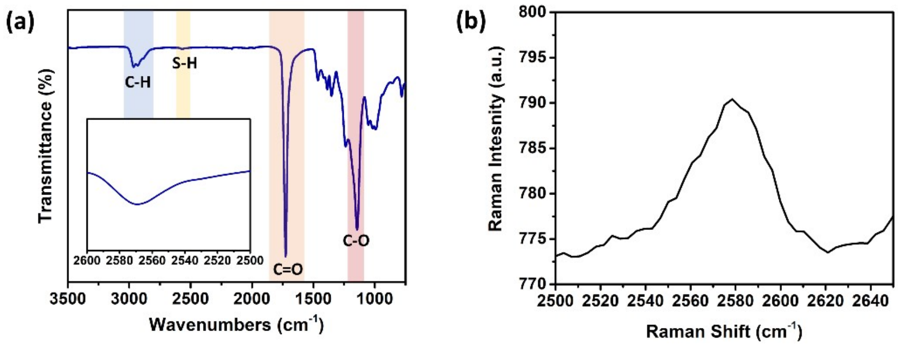

Fig. S1 (a) FTIR spectrum of (SH)polyHIPE substrate (Referred standard data: (i) C-H stretching: 3000-2849 cm^{-1}; (ii) S-H stretching: 2600-2550 cm^{-1}; (iii) C=O stretching: 1730-1715 cm^{-1}; (iv) C-O stretching: 1210-1163 cm^{-1})[1]; (b) Raman spectrum of (SH)polyHIPE substrate.

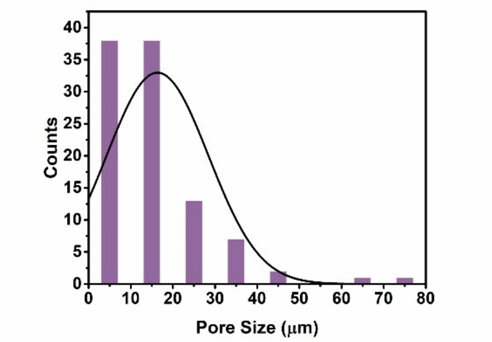

Fig. S2 Pore size distribution of (SH)polyHIPE substrate.

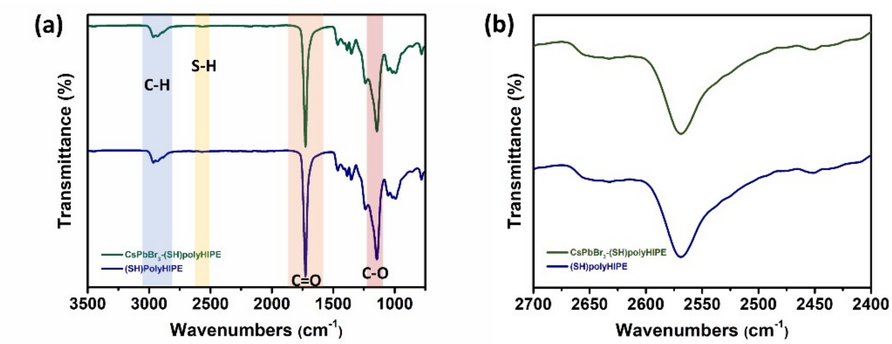

Fig. S3 FTIR spectra of (SH)polyHIPE substrate and $CsPbBr_3$-(SH)polyHIPE composite: (a) The entire spectra; (b) The partially enlarged spectra

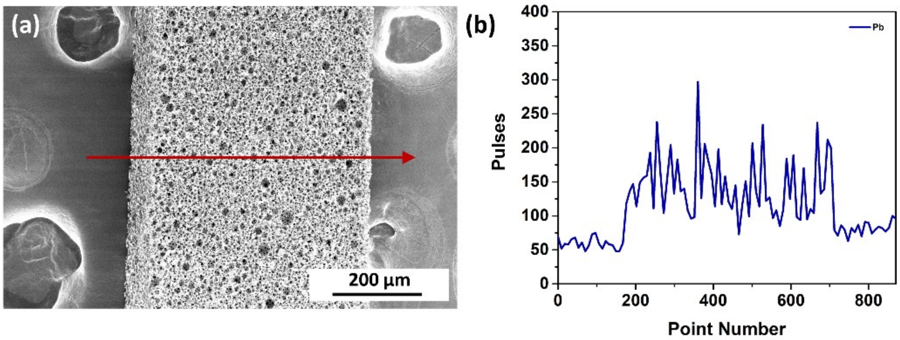

Fig. S4 (a) SEM image of cross-sectional $CsPbBr_3$-(SH)polyHIPE composite; (b) EDS line scan with Pb signal of the cross-sectional surface for $CsPbBr_3$-(SH)polyHIPE composite.

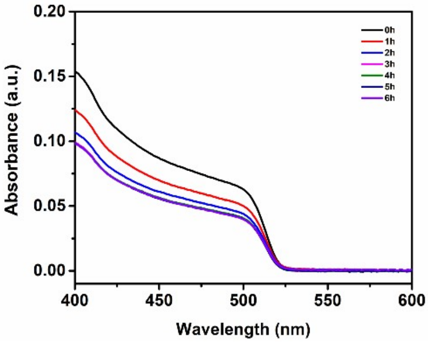

Fig. S5 Absorption spectra of $CsPbBr_3$ NCs colloidal solution during composite fabrication

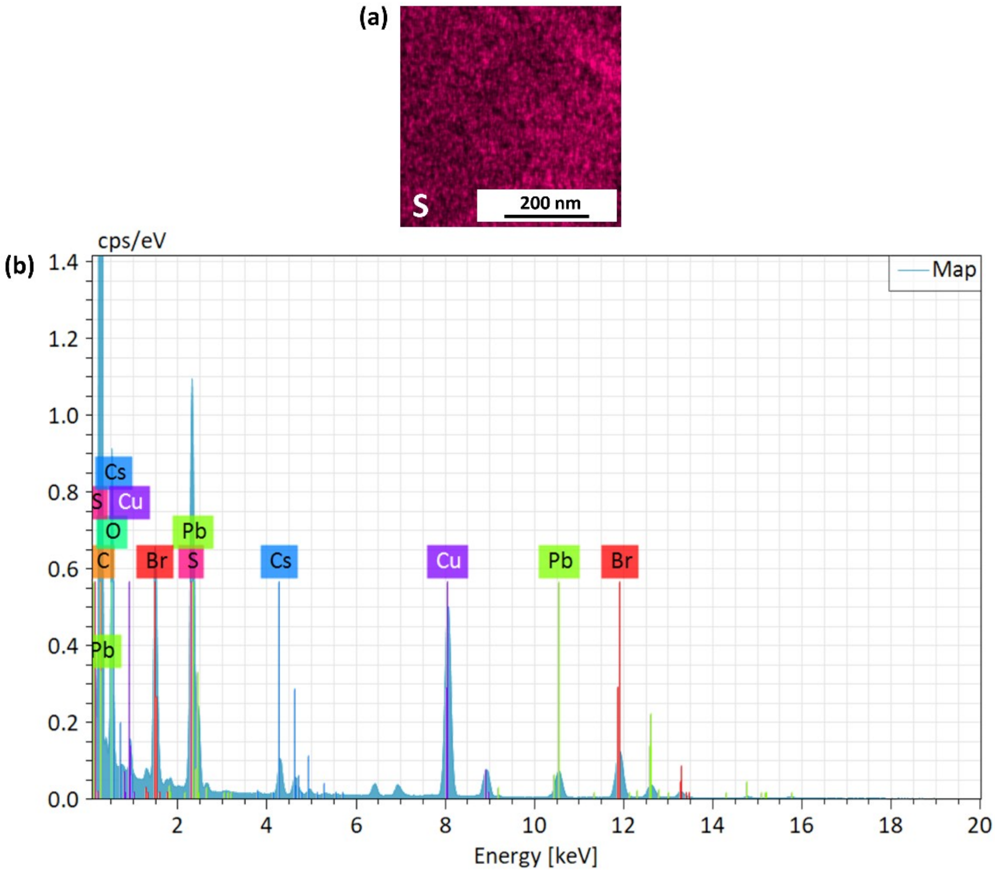

Fig. S6 (a) EDS elemental mapping of S for $CsPbBr_3$-(SH)polyHIPE composite from STEM; (b) EDS spectrum of $CsPbBr_3$-(SH)polyHIPE composite from STEM.

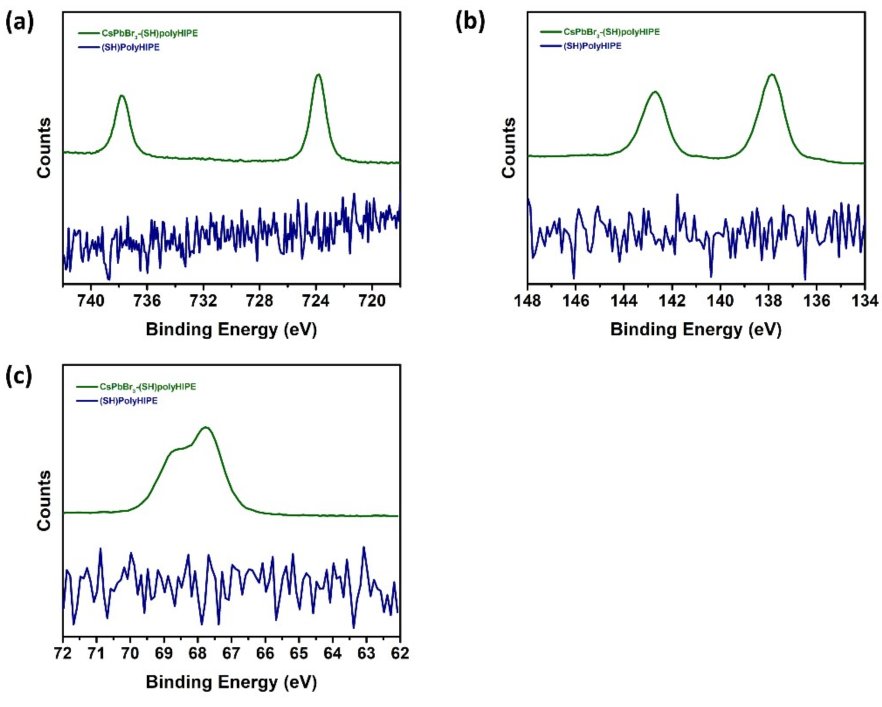

Fig. S7 XPS spectra of (SH)polyHIPE substrate and $CsPbBr_3$-(SH)polyHIPE composite. (a) Cs3d spectra of (SH)polyHIPE substrate and $CsPbBr_3$-(SH)polyHIPE composite; (b) Pb4f spectra of

(SH)polyHIPE substrate and $CsPbBr_3$-(SH)polyHIPE composite; (c) Br3d spectra of (SH)polyHIPE substrate and $CsPbBr_3$-(SH)polyHIPE composite.

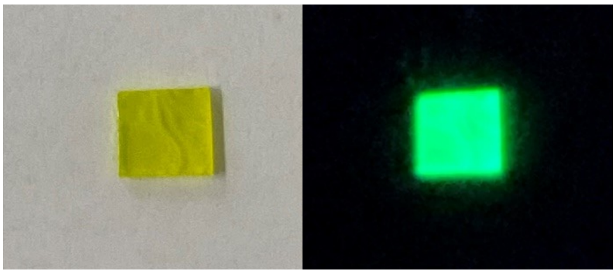

Fig. S8 Photos of $CsPbBr_3$ NCs on the glass substrate (0.5 cm × 0.5 cm) under the room light (left) and 365 nm UV light (right).

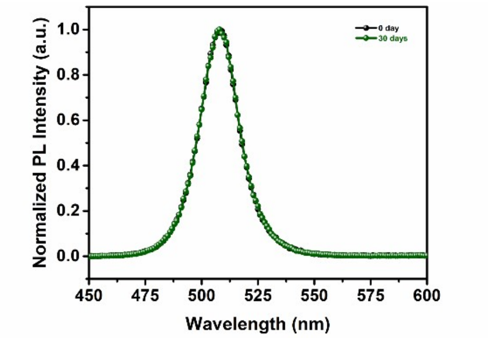

Fig. S9 Normalized PL spectra of $CsPbBr_3$-(SH)polyHIPE composite under the ambient environment for 0 day and 30 days.

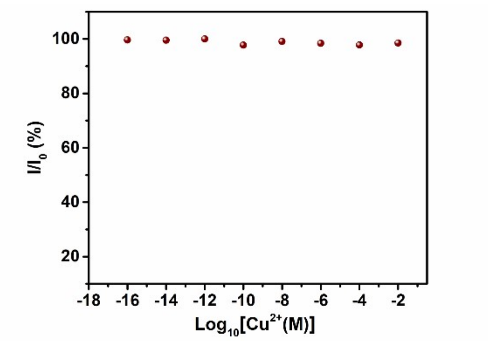

Fig. S10 PL intensity change of $CsPbBr_3$-(SH)polyHIPE composite as a function of the isopycnic blank hexane without Cu^{2+}.

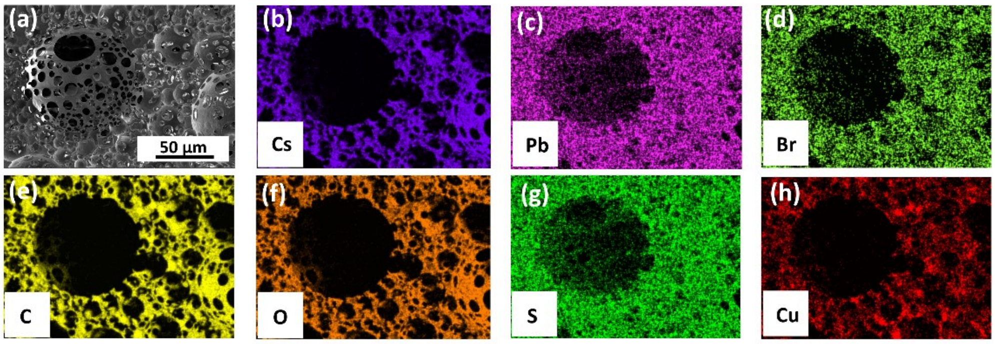

Fig. S11 (a) SEM image of $CsPbBr_3$-(SH)polyHIPE composite after detecting Cu^{2+} with the concentration of 1×10^{-2} M; (b)-(h) EDS mappings of $CsPbBr_3$-(SH)polyHIPE composite after detecting Cu^{2+} with the concentration of 1×10^{-2} M.

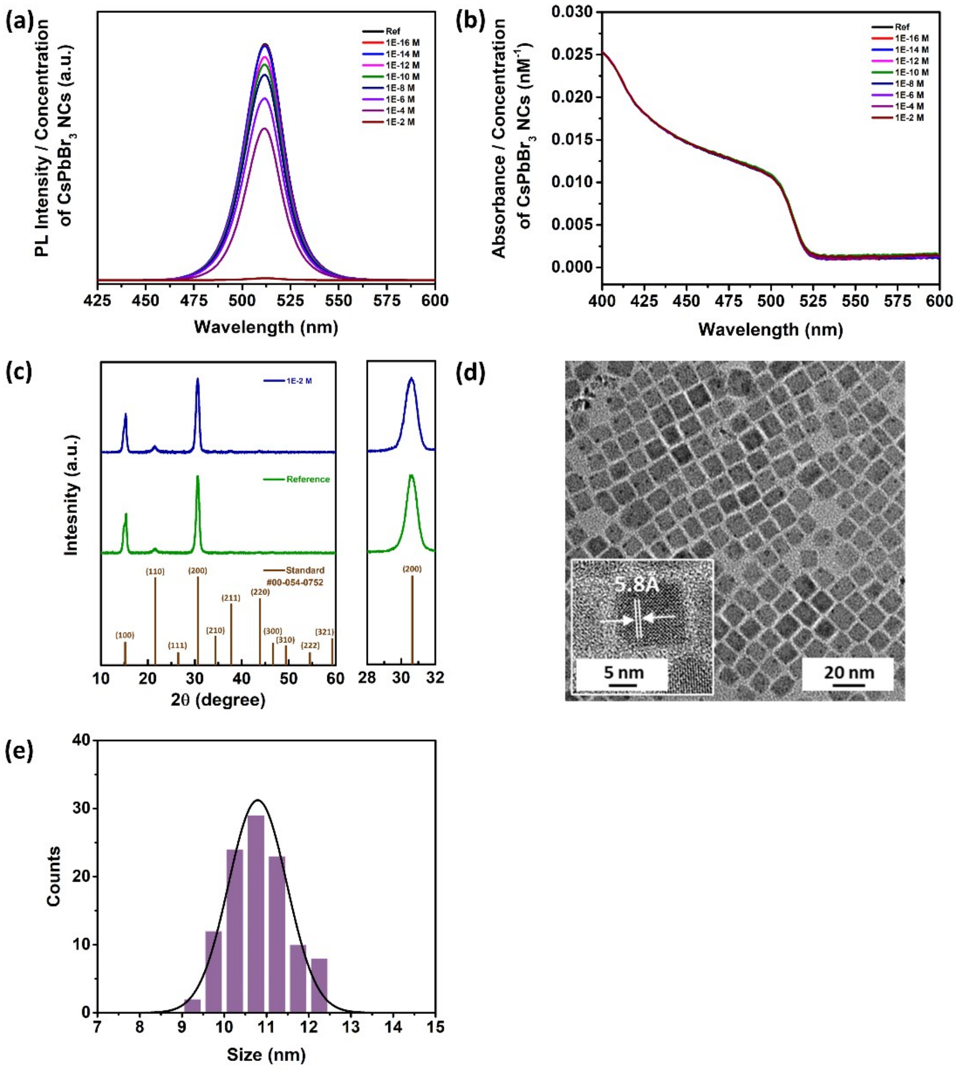

Fig. S12 Characterisation of $CsPbBr_3$ NCs dispersed in hexane for detecting Cu^{2+}; (a) PL spectra of $CsPbBr_3$ NCs for detecting Cu^{2+} with various concentrations; (b) Absorption spectra of $CsPbBr_3$ NCs for detecting Cu^{2+} with various concentrations; (c) XRD of $CsPbBr_3$ NCs before and after detecting Cu^{2+} with the concentration of 1×10^{-2} M; (d) TEM and HRTEM image of $CsPbBr_3$ NCs after detecting

Cu^{2+} + with the concentration of 1×10^{-2} M; (e) Size contribution of $CsPbBr_3$ NCs after detecting Cu^{2+} with the concentration of 1×10^{-2} M.

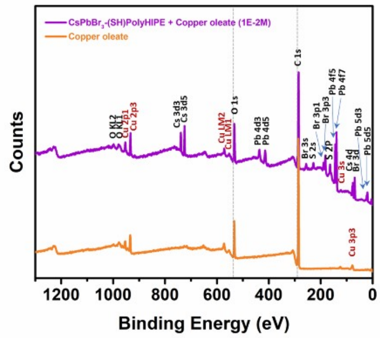

Fig. S13 XPS spectrum of copper oleate and $CsPbBr_3$-(SH)PolyHIPE composite after detecting Cu^{2+} with the concentration of 1×10^{-2} M**.**

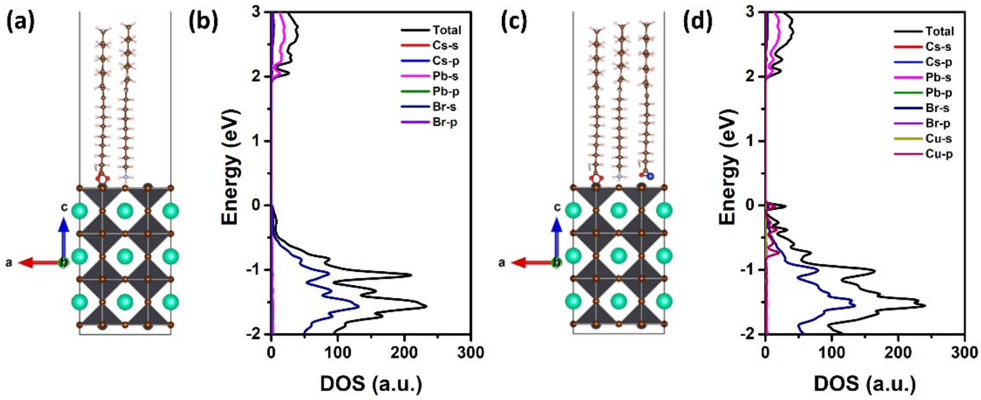

Fig. S14 (a) Schematic figure of $CsPbBr_3$ with oleylammonium and oleate; (b) Density of states of $CsPbBr_3$ with oleylammonium and oleate; (c) Schematic figure of $CsPbBr_3$ with oleylammonium, oleate and Cu(oleate); (d) Density of states of $CsPbBr_3$ with oleylammonium, oleate and Cu(oleate).

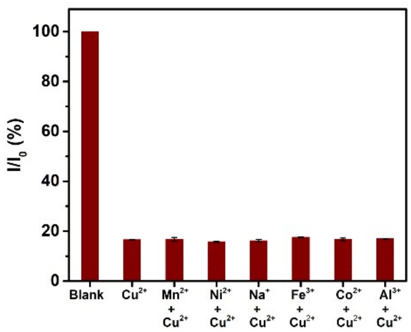

Fig. S15 PL intensity change of $CsPbBr_3$-(SH)polyHIPE composite to bi-mixed metal ions. The concentration of each metal ion is 1×10^{-2} M.

2. Tables

Table S1. XPS results of as-prepared $CsPbBr_3$-(SH)polyHIPE composite

Element	Atomic %
Cs3d	17.61
Pb4f	20.08
Br3d	62.31

Table S2. Summary of PL spectra analysis of $CsPbBr_3$ NCs in hexane, $CsPbBr_3$-(SH)polyHIPE composite, $CsPbBr_3$ on glass substrate

Material	Peak Position	Full width at half maximum (FWHM)
$CsPbBr_3$ in hexane	512 nm	24 nm
$CsPbBr_3$-(SH)polyHIPE	514 nm	22 nm
$CsPbBr_3$ on glass substrate	518 nm	27 nm

Table S3. Summary of inorganic nanoparticles for Cu^{2+} detection

Material	Metal format	Limit of detection (LOD)	Reference
BPEI-capped CQDs	Cu^{2+} in water	1.15×10^{-7} M	2
N-doped CQDs	Cu^{2+} in water	2.3×10^{-8} M	3
DDTC- capped CdSe/CdS QDs	Cu^{2+} in water	4.56×10^{-9} M	4
DPA@Cys-CdS QDs	Cu^{2+} in water	3.4×10^{-7} M	5
CTAB-capped CdSe/ZnS QDs	Cu^{2+} in water	1.5×10^{-10} M	6
3-MPA CdSe QDs	Cu^{2+} in water	3×10^{-8} M	7
CdSe@ZIF-8/PAA	Cu^{2+} in water	4×10^{-15} M	8
Thiosulfate-capped Ag/Au NPs	Cu^{2+} in water	1×10^{-9} M	9

SiO2@Cel -TEPA	Cu^{2+} in water	1.2×10^{-6} M	10
E2MP-capped CdTe	Cu^{2+} in water	5×10^{-10} M	11
$CsPbBr_3$-PMMA membrane	Cu^{2+} in water	1×10^{-15} M	12
$CsPbBr_3$	Cu^{2+} in hexane	1×10^{-10} M	13
$CsPbBr_3$	Cu^{2+} in hexane	2×10^{-9} M	14
$CsPbBr_3$-(SH)polyHIPE	Cu^{2+} in hexane	1×10^{-16} M	This work

Table S4. Fitting results of time-resolved photoluminescence decay of $CsPbBr_3$-(SH)polyHIPE composite by adding various concentrations of Cu^{2+}.

Cu^{2+} Concentration	A_1	τ_1 (ns)	A_2	τ_2 (ns)	$\bar{\tau}$ (ns)
0 M	0.85	4.38	0.15	20.92	11.82
1×10^{-12} M	0.88	3.46	0.12	17.22	8.99
1×10^{-8} M	0.90	3.09	0.10	15.92	7.70
1×10^{-4} M	0.91	2.27	0.09	11.20	5.09

(a) The photoluminescence decay curves were fitted by a bi-exponential function:

$$I(t) = \sum_{i=1}^{2} A_1 exp(-t/\tau_i)$$

(b) The average photoluminescence decay ($\bar{\tau}$) was calculated by:

$$\bar{\tau} = \frac{A_1\tau_1^2 + A_2\tau_2^2}{A_1\tau_1 + A_2\tau_2}$$

3. Calculation

3.1 Calculation of total surface area of a (SH)polyHIPE substrate

Table S5. Average weight of a (SH)polyHIPE substrate

Sample	Weight (mg)	Average Weight (mg)
1	2.7	2.68
2	2.6	
3	2.8	
4	2.7	
5	2.6	

Since the measured surface area of a (SH)polyHIPE substrate is 1.31 m^2/g, the total surface area of a (SH)polyHIPE substrate will be around 3.51×10^9 μm^2.

3.2 Calculation of quantity of $CsPbBr_3$ NCs in hexane during $CsPbBr_3$-(SH)polyHIPE composite fabrication process

The concentration of $CsPbBr_3$ NCs in hexane is calculated based on Beer–Lambert law:

$$A = \epsilon l c$$

A: Absorbance

ϵ: Molar extinction coefficient

l: Optical path length (cm)

c: Concentration of nanoparticles

Specially, the molar extinction coefficient (ϵ) can be determined by the following equation:

$$\epsilon = \frac{N_A \mu_i}{\ln 10} d^3$$

N_A: Avogadro constant

μ_i: Molar absorption coefficient

d: Size of NCs

Table S6. Concentrations of $CsPbBr_3$ NCs in hexane at different time

Time (h)	0	1	2	3	4	5	6
A	0.1544	0.1242	0.10689	0.09919	0.09853	0.09859	0.09829
μ_i (cm^{-1}) [15]	7.7×10^4						
ϵ ($cm^{-1}\cdot\mu M^{-1}$) [15]	$1.98\times10^{-2}\times d^3$						
d (nm)	10.85						

l (cm)	1						
c (nM)	6.11	4.91	4.23	3.92	3.90	3.90	3.89

3.3 Number of $CsPbBr_3$ NCs absorbed on a (SH)polyHIPE substrate

The number (N) of $CsPbBr_3$ NCs absorbed on a (SH)polyHIPE substrate could be calculated:

$$N = \Delta c \times V \times N_A$$

Δc: Change of concentration of $CsPbBr_3$ NCs colloidal solution.

V: Total volume of $CsPbBr_3$ NCs colloidal solution.

N_A: Avogadro constant.

Table S7. Number of $CsPbBr_3$ NCs absorbed on a (SH)polyHIPE substrate

Δc (nM)	2.21
V (ml)	1
N_A	6.02×10^{23}
N	1.33×10^{12}

3.4 Density (D) of $CsPbBr_3$ NCs on a (SH)polyHIPE substrate

The density (D) of $CsPbBr_3$ NCs on a (SH)polyHIPE substrate could be calculated:

$$D = \frac{N}{a_{polyHIPE}}$$

N: number of $CsPbBr_3$ NCs.

$a_{polyHIPE}$: surface area of a (SH)polyHIPE substrate

Table S8. Density (D) of $CsPbBr_3$ NCs on a (SH)polyHIPE substrate

D (#/μm^2)	379

4. References

1 Merck, IR Spectrum Table and Chart, https://www.sigmaaldrich.com/AU/en/technical-documents/technical-article/analytical-chemistry/photometry-and-reflectometry/ir-spectrum-table, (accessed 1 November 2021).

2 Y. Liu, Y. Zhao and Y. Zhang, *Sensors Actuators, B Chem.*, 2014, **196**, 647–652.

3 W. J. Zhang, S. G. Liu, L. Han, H. Q. Luo and N. B. Li, *Sensors Actuators, B Chem.*, 2019, **283**, 215–221.

4 J. Wang, X. Zhou, H. Ma and G. Tao, *Spectrochim. Acta - Part A Mol. Biomol. Spectrosc.*,

2011, **81**, 178–183.

5 K. Ngamdee, K. Chaiendoo, C. Saiyasombat, W. Busayaporn, S. Ittisanronnachai, V. Promarak and W. Ngeontae, *Spectrochim. Acta - Part A Mol. Biomol. Spectrosc.*, 2019, **211**, 313–321.

6 L. H. Jin and C. S. Han, *Anal. Chem.*, 2014, **86**, 7209–7213.

7 S. Jiang, Z. Lu, T. Su, Y. Feng, C. Zhou, P. Hong, S. Sun and C. Li, *Chemosensors*, 2019, **7**, 47.

8 H. Gao, R. Sun, L. He, Z. J. Qian, C. Zhou, P. Hong, S. Sun, R. Mo and C. Li, *ACS Appl. Mater. Interfaces*, 2020, **12**, 4849–4858.

9 T. Lou, L. Chen, Z. Chen, Y. Wang, L. Chen and J. Li, *ACS Appl. Mater. Interfaces*, 2011, **3**, 4215–4220.

10 A. M. Yousif, O. F. Zaid, W. A. El-Said, E. A. Elshehy and I. A. Ibrahim, *Ind. Eng. Chem. Res.*, 2019, **58**, 4828–4837.

11 Y. S. Choudhary and N. Gomathi, *ChemistrySelect*, 2020, **5**, 32–39.

12 Y. Wang, Y. Zhu, J. Huang, J. Cai, J. Zhu, X. Yang, J. Shen and C. Li, *Nanoscale Horizons*, 2017, **2**, 225–232.

13 Y. Liu, X. Tang, T. Zhu, M. Deng, I. P. Ikechukwu, W. Huang, G. Yin, Y. Bai, D. Qu, X. Huang and F. Qiu, *J. Mater. Chem. C*, 2018, **6**, 4793–4799.

14 X. Sheng, Y. Liu, Y. Wang, Y. Li, X. Wang, X. Wang, Z. Dai, J. Bao and X. Xu, *Adv. Mater.*, 2017, **29**, 1–7.

15 J. Maes, L. Balcaen, E. Drijvers, Q. Zhao, J. De Roo, A. Vantomme, F. Vanhaecke, P. Geiregat and Z. Hens, *J. Phys. Chem. Lett.*, 2018, **9**, 3093–3097.